J Math Imaging Vis (2009) 35: 155–164
DOI 10.1007/s10851-009-0161-2

Metrics for 3D Rotations: Comparison and Analysis

Du Q. Huynh

Published online: 18 June 2009

Abstract 3D rotations arise in many computer vision, computer graphics, and robotics problems and evaluation of the distance between two 3D rotations is often an essential task. This paper presents a detailed analysis of six functions for measuring distance between 3D rotations that have been proposed in the literature. Based on the well-developed theory behind 3D rotations, we demonstrate that five of them are bi-invariant metrics on $SO(3)$ but that only four of them are boundedly equivalent to each other. We conclude that it is both spatially and computationally more efficient to use quaternions for 3D rotations. Lastly, by treating the two rotations as a true and an estimated rotation matrix, we illustrate the geometry associated with iso-error measures.

Keywords Matrix Lie group · Lie algebra · Quaternions · 3D rotations · Distance functions

1 Introduction

3D rotations are common entities in many computer vision, computer graphics, and robotics problems that need to deal with the 3D world. Typical applications that involve 3D rotations include the interpolation of trajectory of 3D orientations, robot kinematics, flight simulation, structure from motion, 3D pose recovery of objects, and motion capture. The common issues that arise in these applications are how to efficiently represent 3D rotations and how to correctly evaluate the distance between them. If one of the 3D rotation matrices is a true or reference rotation while the other is an estimated one, then it is useful also to identify regions where identical error measures occur. A few functions for distance measures between 3D rotations have been proposed in the computer vision literature; however, there has neither been detailed analysis provided to these functions nor a comparison of them in the context of the group $SO(3)$ to which 3D rotations belong. The contributions of this paper are: (1) to provide this missing information; (2) to analyze and illustrate the iso-error contours of a given reference rotation.

Rotations in 3D space can be represented in various forms. Euler angles are commonly used in robotics applications where, because of constraints in the design of the joints of robot arms, rotations often have to be carried out in a certain order (e.g., [1]; see also [19]). For other applications where such a constraint is absent, Euler angles are less favoured, precisely because the values of these angles are dependent on the order of rotations about the three principal axes. For research in computer vision and computer graphics, 3D rotations are commonly represented as unit quaternions (e.g., [5, 15, 17, 18]), rotation axes and angles (e.g., [8, 21]), or even as the 3×3 rotation matrices themselves (e.g., [3, 4, 6]). The number of computer vision research papers that involve 3D rotations of any form is far too many to permit a complete list of citations. The references given here are only a very small subset of papers in the literature.

In terms of storage, each 3×3 rotation matrix requires the space of 9 floating point numbers, whereas in reality the special orthogonal group is a 3 dimensional object embeddable in $\mathbb{R}^4$. Another concern of the matrix representation is that after several matrix multiplications, round-off errors within computers can result in "rotation" matrices that are

This research was in part supported by a UWA study leave grant.

D.Q. Huynh (✉)
School of Computer Science and Software Engineering,
The University of Western Australia, Nedlands,
WA 6009, Australia
e-mail: du@csse.uwa.edu.au

no longer orthogonal. In that regard, the unit quaternions are preferred as an alternative way of representing 3D rotations. Although round-off errors may also cause any unit quaternion to have a non-unit magnitude, it is more straightforward to renormalize it to unity in comparison with re-orthogonalizing a distorted matrix.

In the following sections, we will first give a brief overview of the special orthogonal group and the unit quaternions. This is then followed by the formal definition of a distance function or metric. Six different functions for 3D rotations will then be studied in turn; their computation complexity will be briefly analyzed. In Sect. 5, a geometrical interpretation of one of the functions will be studied further, this leads to the discussion on iso-error contours. Finally in Sect. 6, we conclude the paper.

2 $SO(3)$ and Unit Quaternions: An Overview

3D rotations form the so-called Special Orthogonal Group $SO(3)$ of orthogonal matrices with determinant 1. $SO(3)$ is a compact Lie group having the skew-symmetric matrices as its Lie algebra, $so(3)$. This Lie algebra is a non-associative vector space equipped with a binary operation:

$$\begin{aligned} &[\cdot\,,\cdot\,] : so(3) \times so(3) \to so(3), \\ &[\mathbf{A},\mathbf{B}] = \mathbf{AB} - \mathbf{BA} \end{aligned} \tag{1}$$

which can easily be seen to be a closed operation in $so(3)$. The Lie algebra $so(3)$ is the tangent space at the identity element of $SO(3)$. The binary operation defined above is known as the *Lie bracket*, which satisfies the following properties:

$$\begin{aligned} &[\mathbf{A},\mathbf{B}] = -[\mathbf{B},\mathbf{A}], \\ &[\mathbf{A},[\mathbf{B},\mathbf{C}]] + [\mathbf{C},[\mathbf{A},\mathbf{B}]] + [\mathbf{B},[\mathbf{C},\mathbf{A}]] = 0, \end{aligned} \tag{2}$$

for all $\mathbf{A},\mathbf{B},\mathbf{C} \in so(3)$. It follows immediately from the first property that $[\mathbf{A},\mathbf{A}] = 0$.

In the theory of Lie groups, the exponential map is a mapping from the Lie algebra of a Lie group to the group itself. Such a mapping allows one to recapture the group structure from its Lie algebra. As in the general case of matrix Lie groups, the exponential map $\exp : so(3) \to SO(3)$ is simply:

$$\exp(\mathbf{A}) = \mathbf{I} + \mathbf{A} + \frac{\mathbf{A}^2}{2!} + \frac{\mathbf{A}^3}{3!} + \cdots. \tag{3}$$

For the special orthogonal group $SO(3)$, the exponential map is surjective but not injective. The failure of injectivity is easily seen by considering a skew-symmetric matrix such as

$$\mathbf{A} = \begin{bmatrix} 0 & 1 & 1 \\ -1 & 0 & 1 \\ 1 & -1 & 0 \end{bmatrix} \tag{4}$$

and noting that $\exp(t\mathbf{A}) = \mathbf{I}$ whenever t is an integer multiple of $2\pi/\sqrt{3}$. This example, however, suggests at least some of the degree of non-uniqueness in the exponential parametrization. Indeed, the exponential parametrization of $SO(3)$ corresponds exactly to the rotation axis and rotation angle formulation. Given a rotation with rotation axis $\mathbf{u} = (u_1,u_2,u_3)^\top$ of unit magnitude and rotation angle θ, the 3×3 rotation matrix $\mathbf{R}$ can be obtained by the exponential mapping $\exp([\theta\mathbf{u}]_\times)$, where $[\,\mathbf{a}\,]_\times$ is chosen to be the matrix defined by $[\mathbf{a}]_\times\mathbf{b} = \mathbf{a}\times\mathbf{b}$. For example, the matrix in (4) corresponds to $[(-1,1,-1)]_\times$. The group $SO(3)$ is covered by one-parameter groups (in fact circles) of the form $\{\exp([\theta\mathbf{u}]_\times) : \theta \in [-\pi,\pi)\}$ and this representation is almost unique, since a rotation uniquely specifies its (unit vector) rotation axis up to a multiplication by ± 1, and once this is fixed, the angle is specified up to a multiple of 2π.

It is straightforward to show that the Rodrigues formula (see, e.g., [11]) for a rotation matrix $\mathbf{R}$ as defined below

$$\mathbf{R} = \cos\theta\,\mathbf{I} + \sin\theta\,[\mathbf{u}]_\times + (1-\cos\theta)\mathbf{u}\mathbf{u}^\top, \tag{5}$$

is just a simplification of the exponential map given in (3) being applied to $[\theta\mathbf{u}]_\times$. Given a 3×3 rotation matrix $\mathbf{R}$, the inverse of the exponential map provides *a* rotation angle/axis description of the rotation. Thus, $\log(\mathbf{R})$ is the skew-symmetric matrix containing information about the rotation axis and angle. Although the inverse process requires a choice of rotation axis between the two alternatives, it is a straightforward procedure to retrieve the rotation axis and angle (see Appendix A).

As a unit quaternion, the same 3D rotation matrix $\exp([\theta\mathbf{u}]_\times) \in SO(3)$ can be written as $\mathbf{q} \equiv (q_0,q_1,q_2,q_3)^\top \equiv (q_0,\tilde{\mathbf{q}})^\top$
$= \pm(\cos\frac{\theta}{2}, \mathbf{u}^\top \sin\frac{\theta}{2})^\top$. The unit quaternions are a one-to-one parametrization of the Special Unitary group $SU(2)$ and the $\mathbf{q}$ above can be written as a 2×2 unitary matrix:

$$\begin{bmatrix} q_0 + iq_1 & q_2 + iq_3 \\ -q_2 + iq_3 & q_0 - iq_1 \end{bmatrix}. \tag{6}$$

$SU(2)$ provides a double-covering of $SO(3)$; that is, each rotation matrix in $SO(3)$ corresponds to two members of $SU(2)$. The group homomorphism from $SU(2)$ to $SO(3)$ has a two element kernel and this corresponds to the ambiguity in the choice of rotation axis in the logarithmic map. In this regard, we note that $SU(2)$ and $SO(3)$ have the same Lie algebra. The Lie algebra $su(2)$, which consists of the 2×2 skew-hermitian matrices, is isomorphic as a Lie algebra to $so(3)$. Consider representing the rotation axis $\mathbf{u} = (u_1,u_2,u_3)^\top$ of unit magnitude and the rotation angle θ as a 2×2 skew-hermitian matrix, $\mathbf{A}$, as follows:

$$\mathbf{A} = \begin{bmatrix} i\theta u_1 & \theta u_2 + i\theta u_3 \\ -\theta u_2 + i\theta u_3 & -i\theta u_1 \end{bmatrix}$$

$$= \theta \begin{bmatrix} iu_1 & u_2 + iu_3 \\ -u_2 + iu_3 & -iu_1 \end{bmatrix} \equiv \theta \tilde{\mathbf{A}}. \tag{7}$$

By applying the exponential mapping to $\mathbf{A}$ and noting that $\mathbf{A}^2 = -\theta^2 \mathbf{I}$, we obtain a different version of the Rodrigues formula:

$$\exp : su(2) \to SU(2),$$

$$\exp(\mathbf{A}) = \cos\theta\, \mathbf{I} + \frac{\sin\theta}{\theta}\mathbf{A} \tag{8}$$

$$= \cos\theta\, \mathbf{I} + \sin\theta\, \tilde{\mathbf{A}}.$$

It is straightforward to verify that $\exp(\mathbf{A}) \in SU(2)$ and that the quaternions are simply a parametrization of $SU(2)$. The exponential map from $su(2)$ to $SU(2)$ does not suffer from the ambiguity present in the orthogonal case.

3 Distance Function or Metric

3.1 Definition

For definiteness, we give the usual definition of *distance function* or *metric*. Let S be some space between whose elements we are interested in knowing distances. A *distance function or metric* is a map $\Phi : S \times S \to \mathbb{R}^+$ satisfying the usual axioms for metrics:

(i) $\Phi(x, y) = 0 \Leftrightarrow x = y$;
(ii) $\Phi(x, y) = \Phi(y, x)$ for $x, y \in S$;
(iii) $\Phi(x, z) \leq \Phi(x, y) + \Phi(y, z)$ for $x, y, z \in S$.

We note that there are situations where our intuitive concept of "distance" may not satisfy these axioms.

There are two other properties of distance functions that are important in the context of $SO(3)$. The first is that the distance function defines and respects the topology of $SO(3)$. To state precisely what this means, we note that the obvious definition of $\mathbf{R}_n \to \mathbf{R}$ as $n \to \infty$ for $\mathbf{R}_n, \mathbf{R} \in SO(3)$ is that the matrix entries of the $\mathbf{R}_n$ should converge to the matrix entries of $\mathbf{R}$ as real numbers. We say that a distance function Φ respects the topology of $SO(3)$ provided

$$\Phi(\mathbf{R}_n, \mathbf{R}) \to 0 \quad \Leftrightarrow \quad \mathbf{R}_n \to \mathbf{R}. \tag{9}$$

Since $SO(3)$ is compact, it is sufficient [12] that

$$\mathbf{R}_n \to \mathbf{R} \quad \Rightarrow \quad \Phi(\mathbf{R}_n, \mathbf{R}) \to 0. \tag{10}$$

It is essential that this is the case for all distance functions defined on $SO(3)$.

Since $SO(3)$ is a group, we can ask one other property of interest. We say that a distance function Φ is *left, (resp. right) invariant* if

$$\Phi(\mathbf{R}_1\mathbf{R}_2, \mathbf{R}_1\mathbf{R}_3) = \Phi(\mathbf{R}_2, \mathbf{R}_3), \tag{11}$$

$$\big(\text{resp. } \Phi(\mathbf{R}_2\mathbf{R}_1, \mathbf{R}_3\mathbf{R}_1) = \Phi(\mathbf{R}_2, \mathbf{R}_3)\big) \tag{12}$$

for $\mathbf{R}_1, \mathbf{R}_2, \mathbf{R}_3 \in SO(3)$. A distance function is *bi-invariant* if it is both left and right invariant.

Two distance functions Φ and Ψ are said to be *boundedly equivalent* if there are positive real numbers a and b such that

$$a\Phi(\mathbf{R}_1, \mathbf{R}_2) \leq \Psi(\mathbf{R}_1, \mathbf{R}_2) \leq b\Phi(\mathbf{R}_1, \mathbf{R}_2) \tag{13}$$

for all $\mathbf{R}_1$, $\mathbf{R}_2 \in SO(3)$. We also define *functional equivalence* between Φ and Ψ to mean that there exists a positive continuous strictly increasing function h such that

$$h \circ \Phi = \Psi. \tag{14}$$

It is easy to see that if one distance function respects the topology of $SO(3)$ and another is either boundedly or functionally equivalent to it then it too respects the topology. Also, if Φ is a distance function satisfying

$$c\Phi(\mathbf{R}_1, \mathbf{R}_2) \leq \Phi(\mathbf{R}\mathbf{R}_1, \mathbf{R}\mathbf{R}_2) \leq d\Phi(\mathbf{R}_1, \mathbf{R}_2) \tag{15}$$

for all $\mathbf{R}_1, \mathbf{R}_2, \mathbf{R} \in SO(3)$ and for some positive real numbers c and d, then it is equivalent to a left-invariant one. The invariant distance function is

$$\Phi_L(\mathbf{R}_1, \mathbf{R}_2) = \int \Phi(\mathbf{R}\mathbf{R}_1, \mathbf{R}\mathbf{R}_2)\, d\mathbf{R} \tag{16}$$

for all $\mathbf{R}_1, \mathbf{R}_2 \in SO(3)$ where the integral is with respect to the (left) Haar measure on the group. We note that this measure is left invariant and it is this property which ensures left invariance of the distance function. A similar result holds for right and bi-invariant distance functions. Note that, in this case, since $SO(3)$ is a compact group its left and right Haar measures are the same.

Finally, two metrics are said to be *topologically equivalent* if they give the same convergent sequences. Both *functional* and *bounded equivalence* individually imply *topological equivalence*. Our assumption that metrics respect the topology means that they are topologically equivalent to each other.

Several functions for measuring the *distance* between two 3D rotations for various applications have been reported in the literature. Some of these functions are defined in terms of Euler angles or quaternions, while others involve the rotation matrices. We will discuss each of them in turn below. We assume that the two rotation matrices whose distance is of interest are $\mathbf{R}_1 = \exp([\theta_1 \mathbf{u}]_\times)$ and $\mathbf{R}_2 = \exp([\theta_2 \mathbf{v}]_\times)$, where θ_1 and θ_2 are the rotation angles, and $\mathbf{u}$ and $\mathbf{v}$ the rotation axes of unit magnitude. Their corresponding unit quaternions can be written as $\mathbf{q}_1 = \pm(\cos\frac{\theta_1}{2}, \mathbf{u}^\top \sin\frac{\theta_1}{2})^\top$ and $\mathbf{q}_2 = \pm(\cos\frac{\theta_2}{2}, \mathbf{v}^\top \sin\frac{\theta_2}{2})^\top$, respectively. All rotation axes are assumed to be of unit magnitude from here on.

3.2 Euclidean Distance between the Euler Angles

Let $(\alpha_1, \beta_1, \gamma_1)$ and $(\alpha_2, \beta_2, \gamma_2)$ be two sets of Euler angles. Then

$$\begin{aligned} &\Phi_1 : E \times E \to \mathbb{R}^+, \\ &\Phi_1((\alpha_1, \beta_1, \gamma_1), (\alpha_2, \beta_2, \gamma_2)) \\ &\quad = \sqrt{d(\alpha_1, \alpha_2)^2 + d(\beta_1, \beta_2)^2 + d(\gamma_1, \gamma_2)^2}, \end{aligned} \tag{17}$$

where $E \subset \mathbb{R}^3$ is an appropriate domain for the three Euler angles (see the discussion that follows) and $d(a, b) = \min\{|a - b|, 2\pi - |a - b|\}$ denotes the normalized difference between the two angles so that $0 \le d(.,.) \le \pi$. The range of values of Φ_1 is $[0, \pi\sqrt{3}]$. This function was discussed in [9] in the context of rotation matrix sampling. Unfortunately, it is not a distance function on $SO(3)$ since it depends on a representation that is not unique. For example, the Euler angles $(\alpha, \beta, \gamma) = (\pi, \pi, 0)$ can represent the same rotation as $(\alpha, \beta, \gamma) = (0, 0, \pi)$ under a particular order of rotations, yet their distance is non-zero. To overcome the problem of ambiguous representation, we can impose the following conditions on the Euler angles (and thus the domain E): $\alpha, \gamma \in [-\pi, \pi)$; $\beta \in [-\pi/2, \pi/2)$. Under this representation, Φ_1 is a metric on $SO(3)$.

3.3 Norm of the Difference of Quaternions

Ravani and Roth [16] define the distance between two rotations as the Euclidean distance between two unit quaternions. As unit quaternions $\mathbf{q}$ and $-\mathbf{q}$ denote the same rotation, we can define the following function, which takes into account the ambiguity in quaternion representation:

$$\begin{aligned} &\Phi_2 : S^3 \times S^3 \to \mathbb{R}^+, \\ &\Phi_2(\mathbf{q}_1, \mathbf{q}_2) = \min\{\|\mathbf{q}_1 - \mathbf{q}_2\|, \|\mathbf{q}_1 + \mathbf{q}_2\|\}, \end{aligned} \tag{18}$$

where $\|\cdot\|$ denotes the Euclidean norm (or 2-norm) and $S^3 = \{\mathbf{q} \in \mathbb{R}^4 \mid \|\mathbf{q}\|^2 = 1\}$. We can easily verify that in the S^3 space, the Φ_2 function above satisfies all axioms except for Axiom (i) since $\Phi_2(\mathbf{q}, -\mathbf{q}) = 0 \not\Rightarrow \mathbf{q} = -\mathbf{q}$ (as vectors in $\mathbb{R}^4$). This means that Φ_2 is a *pseudometric* [7] rather than a metric on the unit quaternions. However, as the mapping from unit quaternions to $SO(3)$ is 2-to-1, the pseudometric on the unit quaternions becomes a metric on 3D rotations because we are identifying points with zero distance apart.

The Φ_2 metric gives values in the range $[0, \sqrt{2}]$.

3.4 Inner Product of Unit Quaternions

A similar function that involves unit quaternions is given by:

$$\begin{aligned} &\Phi_3' : S^3 \times S^3 \to \mathbb{R}^+, \\ &\Phi_3'(\mathbf{q}_1, \mathbf{q}_2) = \min\{\arccos(\mathbf{q}_1 \cdot \mathbf{q}_2), \pi - \arccos(\mathbf{q}_1 \cdot \mathbf{q}_2)\}, \end{aligned}$$

where $\cdot$ denotes the inner (or dot) product of vectors (not the quaternion multiplication, which produces another quaternion). This function was used by Wunsch et al. [20] for 3D object pose estimation. As in (18), the ambiguity in sign of unit quaternions must be taken into consideration. So, Φ_3' can be replaced by the following computationally more efficient function:

$$\begin{aligned} &\Phi_3 : S^3 \times S^3 \to \mathbb{R}^+, \\ &\Phi_3(\mathbf{q}_1, \mathbf{q}_2) = \arccos(|\mathbf{q}_1 \cdot \mathbf{q}_2|). \end{aligned} \tag{19}$$

Since it is necessary that Φ_3 is a non-negative function, we restrict the angles returned by arccos to be in the first quadrant, i.e., the range of values mapped by Φ_3 is $[0, \pi/2]$ (radians).

Alternatively, the inverse cosine function above can be eliminated by defining

$$\begin{aligned} &\Phi_4 : S^3 \times S^3 \to \mathbb{R}^+, \\ &\Phi_4(\mathbf{q}_1, \mathbf{q}_2) = 1 - |\mathbf{q}_1 \cdot \mathbf{q}_2|. \end{aligned} \tag{20}$$

This function was used in [9] for the distance measure between two Euclidean transformations. Function Φ_4 give values in the range [0, 1].

Following the same argument as that for Φ_2, we can conclude that both Φ_3 and Φ_4 are pseudometrics on the unit quaternions but are metrics on $SO(3)$. Up to this point, we have not discussed whether Φ_2, Φ_3, and Φ_4 are bi-invariant metrics on $SO(3)$. We defer the proof for this until later in the paper.

3.5 Deviation from the Identity Matrix

Larochelle et al. [10] use polar decomposition to approximate elements of the Euclidean group $SE(n-1)$ with elements of the special orthogonal group $SO(n)$ and then employ the metric $d(\mathbf{A}_1, \mathbf{A}_2) = \|\mathbf{I} - \mathbf{A}_1\mathbf{A}_2^\top\|_F$ (where $\mathbf{A}_1, \mathbf{A}_2 \in SO(n)$ and $\|\cdot\|_F$ denotes the Frobenius norm of the matrix) as a distance measure between two rigid body displacements. For the specific case where $n = 3$, we have

$$\begin{aligned} &\Phi_5 : SO(3) \times SO(3) \to \mathbb{R}^+, \\ &\Phi_5(\mathbf{R}_1, \mathbf{R}_2) = \|\mathbf{I} - \mathbf{R}_1\mathbf{R}_2^\top\|_F, \end{aligned} \tag{21}$$

which gives values in the range $[0, 2\sqrt{2}]$. An alternative is to replace the Frobenius norm above by the 2-norm to reduce the range of values to $[0, 2]$ instead.

One can verify that Φ_5 is a metric on $SO(3)$ although the proof to show that the function satisfies the triangle inequality condition involves some messy algebra.

3.6 Geodesic on the Unit Sphere

Since $SO(3)$ is a compact Lie group it has a natural Riemannian metric; that is, an inner product on its tangent space at every point. At the identity, this tangent space is $so(3)$, i.e., the skew-symmetric matrices, as we have mentioned. The inner product on $so(3)$ is given by

$$\langle \mathbf{S}_1, \mathbf{S}_2 \rangle = \frac{1}{2}\text{trace}\left(\mathbf{S}_1^\top \mathbf{S}_2\right), \tag{22}$$

for $\mathbf{S}_1, \mathbf{S}_2 \in so(3)$.

The inner product in the Riemannian structure provides an "infinitesimal" version of length on the tangent vectors, and so the length of a curve can be obtained by integration along the curve. Then the concept of a shortest path between two points on the group, a geodesic, follows. In fact, it is enough to describe the shortest path from the identity of the group to another point which we can write as $\exp(\mathbf{S})$, where $\mathbf{S} \in so(3)$. This shortest path can be shown to be of the form $\exp(t\mathbf{S})$, where $0 \le t \le 1$. We can use this to define a metric on the group by making the distance between two points the length of the geodesic between them. This metric is the one considered by Park and Ravani [13, 14]:

$$\begin{aligned} &\Phi_6 : SO(3) \times SO(3) \to \mathbb{R}^+, \\ &\Phi_6(\mathbf{R}_1, \mathbf{R}_2) = \|\log(\mathbf{R}_1 \mathbf{R}_2^\top)\|, \end{aligned} \tag{23}$$

where, as described above, $\log(\mathbf{R})$ gives the skew-symmetric matrix that embodies the rotation axis and angle of the rotation matrix $\mathbf{R}$. The $\|.\|$ above therefore gives the magnitude of the rotation angle. This Φ_6 function is a bi-invariant metric on $SO(3)$. The proof for this will be given later in the paper. The metric gives values in the range $[0, \pi)$.

It is obvious that both Φ_5 and Φ_6 attempt to find the amount of rotation required to bring $\mathbf{R}_1$ to align with $\mathbf{R}_2$, i.e., to find $\mathbf{R}$ such that $\mathbf{R}_1 = \mathbf{R}\mathbf{R}_2$, thus $\mathbf{R} = \mathbf{R}_1 \mathbf{R}_2^\top$.

4 Comparison of the Metrics

One can verify that all the functions Φ_i, for $i = 1, \ldots, 6$, defined above are metrics on $SO(3)$, although the proof for the triangle inequality condition may not be straightforward for some of them (a proof to show that Φ_6 is a metric is given in Appendix B). It should be noted also that the Φ_1 function does not truly reflect the 'distance' of two rotations. That is, two nearby rotations may have a large Φ_1 value, while two distant rotations may have a smaller Φ_1 value. For this reason, when a distance measure between two rotations is sought, any of the Φ_2 to Φ_6 metrics should be used instead. From here on, the comparison will be focused only on these five metrics.

4.1 Bounded Equivalence

The metrics Φ_i, for $i = 2, \ldots, 6$, produce values in different ranges and of different units: Φ_3 and Φ_6 are in radians while the other three are dimensionless. The difference in units is not an issue as a change of unit merely results in a scale change to the metric being considered. Furthermore, the relationships among these metrics are clearly non-linear, except for Φ_3 and Φ_6. To see that Φ_3 and Φ_6 have a linear relationship, consider the computation of the rotation angle of $\mathbf{R}_1\mathbf{R}_2^\top$ in the definition of Φ_6. As unit quaternions, $\mathbf{R}_1$ and $\mathbf{R}_2^\top$ can be, respectively, represented by $\mathbf{q}_1 = \pm(\cos\frac{\theta_1}{2}, \mathbf{u}^\top \sin\frac{\theta_1}{2})^\top$ and $\bar{\mathbf{q}}_2 = \pm(\cos\frac{\theta_2}{2}, -\mathbf{v}^\top \sin\frac{\theta_2}{2})^\top$, where the overhead bar denotes quaternion conjugate. The cosine of half of the rotation angle of $\mathbf{R}_1\mathbf{R}_2^\top$ can be found from the first component of product $|\mathbf{q}_1\bar{\mathbf{q}}_2|$, which, by definition of quaternion multiplication, is $|\cos\frac{\theta_1}{2}\cos\frac{\theta_2}{2} + \sin\frac{\theta_1}{2}\sin\frac{\theta_2}{2}(\mathbf{u}\cdot\mathbf{v})|$. This term is identical to the absolute value of the dot product of the two 4-vector $\mathbf{q}_1$ and $\mathbf{q}_2$ computed in Φ_3, i.e., $\cos(\frac{\theta}{2}) = |\mathbf{q}_1 \cdot \mathbf{q}_2|$. Thus, Φ_3 returns half of the rotation angle of $\mathbf{R}_1\mathbf{R}_2^\top$ from Φ_6. From the definition given in Sect. 3.1, metrics Φ_3 and Φ_6 are boundedly equivalent.

To prove that two metrics Φ_i and Φ_j are boundedly equivalent (see (13)), it suffices, because $SO(3)$ is compact, to show that Φ_i/Φ_j is bounded near the origin. In particular, the metrics Φ_2 and Φ_5 can be rewritten as

$$\Phi_2(\mathbf{q}_1, \mathbf{q}_2) = \sqrt{2\,(1 - |\mathbf{q}_1 \cdot \mathbf{q}_2|)}, \tag{24}$$

$$\begin{aligned} \Phi_5(\mathbf{R}_1, \mathbf{R}_2) &= \sqrt{\text{trace}\left((\mathbf{I} - \mathbf{R}_1\mathbf{R}_2^\top)^\top(\mathbf{I} - \mathbf{R}_1\mathbf{R}_2^\top)\right)} \\ &= \sqrt{2\,\text{trace}\,(\mathbf{I}) - 2\,\text{trace}\left(\mathbf{R}_1\mathbf{R}_2^\top\right)} \\ &= \sqrt{2\left(3 - \text{trace}\left(\mathbf{R}_1\mathbf{R}_2^\top\right)\right)}. \end{aligned} \tag{25}$$

Let $\mathbf{R}_1\mathbf{R}_2^\top = \exp([\theta\mathbf{u}]_\times)$. Then $\text{trace}\left(\mathbf{R}_1\mathbf{R}_2^\top\right) = 1 + 2\cos(\theta)$ (see Appendix A). Substituting this into (25) gives

$$\Phi_5(\mathbf{R}_1, \mathbf{R}_2) = 2\sqrt{1 - \cos(\theta)} = 2\sqrt{2 - 2\cos^2(\theta/2)}. \tag{26}$$

From the discussion given above, we have $\cos(\theta/2) = |\mathbf{q}_1 \cdot \mathbf{q}_2|$. This gives us an alternative distance function defined in terms of unit quaternions:

$$\begin{aligned} &\Phi_5' : S^3 \times S^3 \to \mathbb{R}^+, \\ &\Phi_5'(\mathbf{q}_1, \mathbf{q}_2) = 2\sqrt{2\,(1 - |\mathbf{q}_1 \cdot \mathbf{q}_2|^2)}. \end{aligned} \tag{27}$$

By taking Φ_3 as the reference metric and applying L'Hôpital's rule, it can be shown that

$$\lim_{|\mathbf{q}_1\cdot\mathbf{q}_2|\to 1} \frac{\Phi_3}{\Phi_2} = \lim_{|\mathbf{q}_1\cdot\mathbf{q}_2|\to 1} \frac{\arccos(|\mathbf{q}_1 \cdot \mathbf{q}_2|)}{\sqrt{2(1 - |\mathbf{q}_1 \cdot \mathbf{q}_2|)}} = 1, \tag{28}$$

$$\lim_{|\mathbf{q}_1\cdot\mathbf{q}_2|\to 1}\frac{\Phi_3}{\Phi_4}=\lim_{|\mathbf{q}_1\cdot\mathbf{q}_2|\to 1}\frac{\arccos(|\mathbf{q}_1\cdot\mathbf{q}_2|)}{1-|\mathbf{q}_1\cdot\mathbf{q}_2|}=\infty, \tag{29}$$

$$\lim_{|\mathbf{q}_1\cdot\mathbf{q}_2|\to 1}\frac{\Phi_3}{\Phi_5}=\lim_{|\mathbf{q}_1\cdot\mathbf{q}_2|\to 1}\frac{\Phi_3}{\Phi_5'}=\lim_{|\mathbf{q}_1\cdot\mathbf{q}_2|\to 1}\frac{\arccos(|\mathbf{q}_1\cdot\mathbf{q}_2|)}{2\sqrt{2(1-|\mathbf{q}_1\cdot\mathbf{q}_2|^2)}}=\frac{1}{2\sqrt{2}}. \tag{30}$$

Thus, Φ_2, Φ_3, Φ_5, and Φ_6 are boundedly equivalent metrics, while Φ_4 is not boundedly equivalent to any other metrics.

4.2 Functional Equivalence

Figure 1 shows the relationships among the five distance functions. The figure was generated using many randomly simulated 3D rotations. The linear relationship between Φ_3 and Φ_6 is evident from the straight green line in the figure. It is also clear that each of the mappings from Φ_i to Φ_j, for $i, j = 2, \ldots, 6, i \neq j$, is a bijection and monotonic increasing. That is, these five metrics are functionally equivalent to each other. Again, taking Φ_3 as the reference metric, one can easily derive that the positive, strictly increasing functions h mapping from Φ_3 to the other four metrics are:

$$\Phi_2 = h_{32}(\Phi_3) \equiv \sqrt{2\,(1-\cos\Phi_3)}, \tag{31}$$

$$\Phi_4 = h_{34}(\Phi_3) \equiv 1-\cos\Phi_3, \tag{32}$$

$$\Phi_5 = h_{35}(\Phi_3) \equiv 2\sqrt{2}\sin\Phi_3, \tag{33}$$

$$\Phi_6 = h_{36}(\Phi_3) \equiv 2\Phi_3. \tag{34}$$

It is interesting to note that the curve for Φ_4 versus Φ_6 approaches the origin approximately quadratically. This indicates that $\Phi_4(\mathbf{q}', \mathbf{q}) \to 0$ at a much slower rate than the other metrics when the rotation represented by $\mathbf{q}'$ approaches the rotation represented by $\mathbf{q}$. This confirms that Φ_4 is not boundedly equivalent to other metrics, as demonstrated earlier.

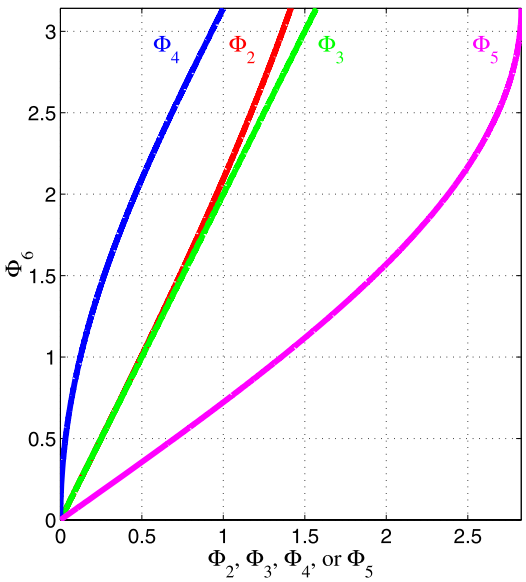

Fig. 1 Metrics Φ_i, for $i = 2, \ldots, 5$ versus Φ_6

If we have a sequence of matrices $\mathbf{R}_n$ such that $\mathbf{R}_n \to \mathbf{R}$ as $n \to \infty$ (Sect. 3.1, (10)), then $\mathbf{R}_n^\top \to \mathbf{R}^\top$ and $\mathbf{R}\mathbf{R}_n^\top \to \mathbf{R}\mathbf{R}^\top = \mathbf{I}$. Using the metric Φ_5 we have

$$\begin{aligned}\Phi_5(\mathbf{R}, \mathbf{R}_n) &= \Phi_5(\mathbf{R}_n, \mathbf{R})\\ &= \|\mathbf{I}-\mathbf{R}_n\mathbf{R}^\top\|_F\\ &\to \|\mathbf{I}-\mathbf{R}\mathbf{R}^\top\|_F\\ &= 0.\end{aligned} \tag{35}$$

Conversely, if $\Phi_5(\mathbf{R}_n, \mathbf{R}) = \Phi_5(\mathbf{R}, \mathbf{R}_n) \to 0$ as $n \to \infty$, then it is necessary that $\mathbf{R}\mathbf{R}_n^\top \to \mathbf{I}$, i.e., $\mathbf{R}_n \to \mathbf{R}$. We can therefore conclude that Φ_5 respects the topology of $SO(3)$, and so do all the metrics Φ_2, Φ_3, Φ_4, and Φ_6, for their functional equivalence to Φ_5.

Table 1 summarizes the computational complexity of these distance functions. Among them, Φ_5 is the most computationally expensive metric. However, the computation work can be significantly reduced if unit quaternions are used instead. Similarly, computation work for function Φ_6

Table 1 Summary of the amount of computations required for each of the distance functions Φ_i, $i = 2, \ldots, 6$. The dot product of two quaternions requires 4 multiplications; the product of two 3×3 rotation matrices require 27 multiplications; the Euclidean norm of a 4-vector requires 4 multiplications; the $\|.\|_F$ norm requires 9 multiplications; to obtain the absolute or minimum value, 1 comparison is required

Function	Range	Computations required
Φ_2	$[0, \sqrt{2}]$	8 multiplications
		1 comparison
Φ_3	$[0, \pi/2]$	4 multiplications
		1 arccos
		1 comparison
Φ_4	$[0, 1]$	4 multiplications
		1 comparison
Φ_5	$[0, 2\sqrt{2}]$	36 multiplications
		1 square root
		Using quaternions (27):
		7 multiplications
		1 square root
Φ_6	$[0, \pi]$	30 multiplications
		1 square root
		1 arccos
		Using quaternion (same as Φ_3):
		4 multiplications
		1 arccos
		1 comparison

can be reduced if rotations are represented as unit quaternions so that the Φ_3 metric can be employed.

5 Further Analysis of Φ_6 and Iso-error Contours

The Φ_6 metric is geometrically more meaningful than the other metrics, as demonstrated from further analysis of the metric given in this section.

Theorem 1 *Let* $\mathbf{R}_1$ *and* $\mathbf{R}_2$ *be two* 3*D rotations. Let* $\mathbf{p}$ *be any arbitrary point on the surface of the unit sphere. Then*

(i) $\Phi_6(\mathbf{R}_1, \mathbf{R}_2) = \max_{\mathbf{p}} \arccos(\mathbf{R}_1\mathbf{p} \cdot \mathbf{R}_2\mathbf{p})$.
(ii) $\hat{\mathbf{p}} = \operatorname{argmax}_{\mathbf{p}} \arccos(\mathbf{R}_1\mathbf{p} \cdot \mathbf{R}_2\mathbf{p}) \Leftrightarrow \hat{\mathbf{p}} \perp$ *rotation axis of* $\mathbf{R}_1^\top\mathbf{R}_2$.

Proof The proofs for (i) and (ii) can be combined. Consider $\mathbf{R}_1\mathbf{p} \cdot \mathbf{R}_2\mathbf{p}$. We have $\mathbf{R}_1\mathbf{p} \cdot \mathbf{R}_2\mathbf{p} = \mathbf{p}^\top(\mathbf{R}_1^\top\mathbf{R}_2)\mathbf{p}$. Let $\mathbf{R}_1^\top\mathbf{R}_2 = \exp([\mathbf{w}\beta]_\times)$ for some rotation angle β and rotation axis $\mathbf{w}$. By treating $\mathbf{p}$ as a vector of the unit sphere and expressing $\mathbf{p}$ as the sum of two component vectors, one parallel and another orthogonal to $\mathbf{w}$, we see that clearly, if $\mathbf{p}$ is parallel to the rotation axis $\mathbf{w}$, it is invariant under the rotation, so $\mathbf{p}^\top \exp([\mathbf{w}\beta]_\times)\mathbf{p} = \mathbf{p}^\top\mathbf{p} = 1$ and $\arccos(\mathbf{R}_1\mathbf{p} \cdot \mathbf{R}_2\mathbf{p})$ attains the minimum value 0. If $\mathbf{p}$ is orthogonal to $\mathbf{w}$, then $\mathbf{p}^\top \exp([\mathbf{w}\beta]_\times)\mathbf{p} = \cos\beta$ and $\arccos(\mathbf{R}_1\mathbf{p} \cdot \mathbf{R}_2\mathbf{p})$ attains its maximum value β. Following the same argument, we can conclude that if $\arccos(\mathbf{R}_1\hat{\mathbf{p}} \cdot \mathbf{R}_2\hat{\mathbf{p}}) = \beta$, for any $\hat{\mathbf{p}}$, then it is necessary that $\hat{\mathbf{p}}$ is orthogonal to the rotation axis of $\mathbf{R}_1^\top\mathbf{R}_2$.

What remains to be proven is $\Phi_6(\mathbf{R}_1, \mathbf{R}_2) = \beta$. This can be easily seen by considering the dot product of any two unit quaternions $\mathbf{q}_1$ and $\mathbf{q}_2$ associated with $\mathbf{R}_1$ and $\mathbf{R}_2$. Since $|\bar{\mathbf{q}}_1 \cdot \mathbf{q}_2|$ and $|\mathbf{q}_1 \cdot \bar{\mathbf{q}}_2|$ are, respectively, the cosine of half of the rotation angle β of $\mathbf{R}_1^\top\mathbf{R}_2$ and the cosine of half of the rotation angle of $\mathbf{R}_1\mathbf{R}_2^\top$, the equality of $|\bar{\mathbf{q}}_1 \cdot \mathbf{q}_2|$ and $|\bar{\mathbf{q}}_1 \cdot \mathbf{q}_2|$ means that $\Phi_6(\mathbf{R}_1, \mathbf{R}_2) = \beta = \max_{\mathbf{p}} \arccos(\mathbf{R}_1\mathbf{p} \cdot \mathbf{R}_2\mathbf{p})$. □

The above theorem shows that Φ_6 gives the maximum angular measure of separation of points transformed by the two rotations. The following corollary is immediate.

Corollary 1 *Given any two* 3*D rotations* $\mathbf{R}_1$ *and* $\mathbf{R}_2$, *all the rotations* $\mathbf{R}_1\mathbf{R}_2^\top$, $\mathbf{R}_1^\top\mathbf{R}_2$, $\mathbf{R}_2\mathbf{R}_1^\top$, *and* $\mathbf{R}_2^\top\mathbf{R}_1$ *have the same rotation angle.*

Theorem 2 Φ_6 *is a bi-invariant metric on* $SO(3)$.

Proof It is easy to verify that Φ_6 is right-invariant as for any rotation matrices $\mathbf{R}_1$, $\mathbf{R}_2$, and $\mathbf{R}$, we have

$$\begin{aligned}\Phi_6(\mathbf{R}_1\mathbf{R}, \mathbf{R}_2\mathbf{R}) &= \|\log(\mathbf{R}_1\mathbf{R}(\mathbf{R}_2\mathbf{R})^\top)\| \\ &= \|\log(\mathbf{R}_1\mathbf{R}\mathbf{R}^\top\mathbf{R}_2^\top)\| \\ &= \|\log(\mathbf{R}_1\mathbf{R}_2^\top)\| = \Phi_6(\mathbf{R}_1, \mathbf{R}_2).\end{aligned}$$

To show that Φ_6 is left-invariant also, we may apply Corollary 1 above. Given the same three arbitrary rotation matrices, we have

$$\begin{aligned}\Phi_6(\mathbf{R}\mathbf{R}_1, \mathbf{R}\mathbf{R}_2) &= \|\log(\mathbf{R}\mathbf{R}_1(\mathbf{R}\mathbf{R}_2)^\top)\| \\ &= \|\log((\mathbf{R}\mathbf{R}_2)^\top\mathbf{R}\mathbf{R}_1)\| \\ &= \|\log(\mathbf{R}_2^\top\mathbf{R}^\top\mathbf{R}\mathbf{R}_1)\| \\ &= \|\log(\mathbf{R}_2^\top\mathbf{R}_1)\| \\ &= \|\log(\mathbf{R}_1\mathbf{R}_2^\top)\| = \Phi_6(\mathbf{R}_1, \mathbf{R}_2).\end{aligned}$$

Φ_6 is thus a bi-invariant metric on $SO(3)$. □

The functional equivalence of the metrics Φ_i, for $i = 2, \ldots, 6$, means that all of these five metrics are bi-invariant.

Theorem 3 *Let* $\mathbf{R}_0 = \exp([\theta_0\mathbf{u}]_\times)$, $\mathbf{R}_1 = \exp([\theta_1\mathbf{v}]_\times)$, *and* $\mathbf{R}_2 = \exp([\theta_1\mathbf{w}]_\times)$. *Then* $\Phi_6(\mathbf{R}_0, \mathbf{R}_1) = \Phi_6(\mathbf{R}_0, \mathbf{R}_2)$ *iff* $\mathbf{u} \cdot \mathbf{v} = \mathbf{u} \cdot \mathbf{w}$.

Proof The three rotations can be written in unit quaternions as follows: $\mathbf{q}_0 = (\cos\frac{\theta_0}{2}, \mathbf{u}^\top \sin\frac{\theta_0}{2})^\top$, $\mathbf{q}_1 = (\cos\frac{\theta_1}{2}, \mathbf{v}^\top \sin\frac{\theta_1}{2})^\top$, $\mathbf{q}_2 = (\cos\frac{\theta_1}{2}, \mathbf{w}^\top \sin\frac{\theta_1}{2})^\top$. We have

$$\begin{aligned}&\Phi_6(\mathbf{R}_0, \mathbf{R}_1) = \Phi_6(\mathbf{R}_0, \mathbf{R}_2) \\ \Leftrightarrow\quad &\mathbf{q}_1\bar{\mathbf{q}}_0 \text{ and } \mathbf{q}_2\bar{\mathbf{q}}_0 \text{ have the same rotation angle} \\ \Leftrightarrow\quad &\mathbf{q}_1 \cdot \bar{\mathbf{q}}_0 = \mathbf{q}_2 \cdot \bar{\mathbf{q}}_0 \\ \Leftrightarrow\quad &\cos\frac{\theta_1}{2}\cos\frac{\theta_0}{2} + \sin\frac{\theta_1}{2}\sin\frac{\theta_0}{2}(\mathbf{u} \cdot \mathbf{v}) \\ &\quad = \cos\frac{\theta_1}{2}\cos\frac{\theta_0}{2} + \sin\frac{\theta_1}{2}\sin\frac{\theta_0}{2}(\mathbf{u} \cdot \mathbf{w}) \\ \Leftrightarrow\quad &\mathbf{u} \cdot \mathbf{v} = \mathbf{u} \cdot \mathbf{w}.\end{aligned}$$

□

Corollary 2 *The locus of all the rotation matrices,* $\mathbf{R}$, *which have the same rotation angle and are equidistant from a reference rotation* $\mathbf{R}_0 = \exp([\theta_0\mathbf{w}]_\times)$, *is a cone with central axis* $\mathbf{w}$.

In plain English, Theorem 3 and Corollary 2 state that if two different rotations have the same rotation angle and are equidistant from a reference rotation, then their rotation axes must deviate by the same amount from the rotation axis of the reference rotation.

5.1 Iso-error Contours

Consider the rotations $\mathbf{R}_0 = \exp([\theta_0\mathbf{u}]_\times)$ and $\mathbf{R}_1 = \exp([\theta_1\mathbf{v}]_\times)$ given in Theorem 3 again. If $\mathbf{R}_0$ is the true rotation and $\mathbf{R}_1$ is an estimated rotation, then the distance measure $\Phi_6(\mathbf{R}_0, \mathbf{R}_1)$ can be taken as an error measure of $\mathbf{R}_1$.

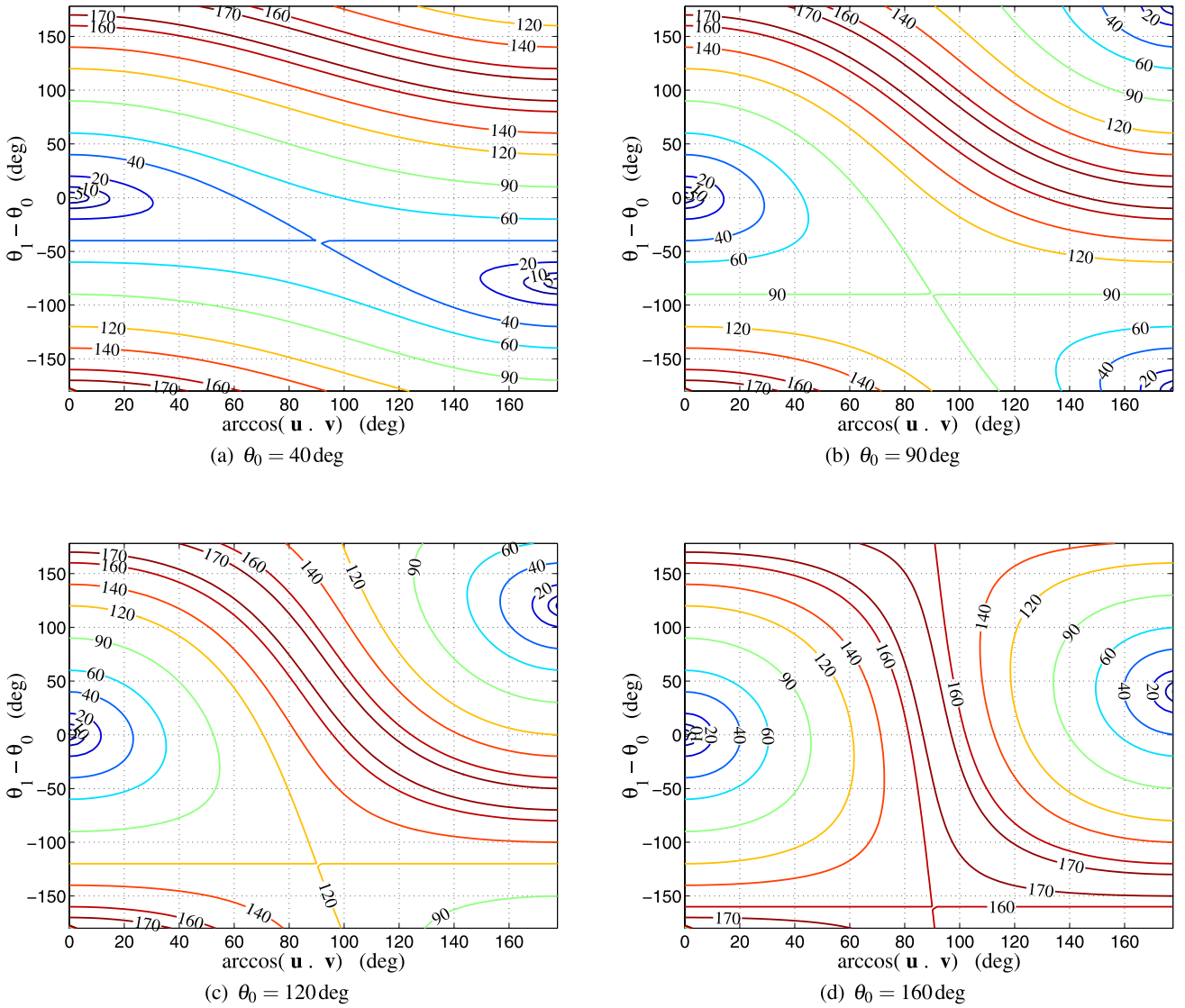

Fig. 2 Error-contour plots of a 3D rotation $\mathbf{R}_1 = \exp([\theta_1 \mathbf{v}]_\times)$ for different values of the rotation angle θ_0 of the true rotation, $\mathbf{R}_0 = \exp([\theta_0 \mathbf{u}]_\times)$. In each plot, the *horizontal axis* corresponds to $\arccos(\mathbf{u} \cdot \mathbf{v})$, i.e., the angle of deviation between the two rotation axes of $\mathbf{R}_0$ and $\mathbf{R}_1$; the *vertical axis* corresponds to the difference of the rotation angles, i.e., $\theta_1 - \theta_0$. Both axes are in degrees

Of interest is then the geometry of the set of rotations that are on the iso-error contours. From Theorem 3 and Corollary 2, we see that $\mathbf{R}_1$ is on the iso-error contour with all the matrices in the set $\{\mathbf{R} = \exp([\theta_1 \mathbf{w}]_\times) \mid \mathbf{u} \cdot \mathbf{v} = \mathbf{u} \cdot \mathbf{w}\}$. However, there are other rotation matrices outside this set having the same error measure from $\mathbf{R}_0$ also. If we start altering the direction of the rotation axis $\mathbf{v}$ to increase its angle of deviation with $\mathbf{u}$ (this corresponds to decreasing $\mathbf{u} \cdot \mathbf{v}$), then it would be necessary that the difference between θ_0 and θ_1 be adjusted in order to have $\mathbf{R}_1$ still remain on the same error contour. The induced change to the difference between θ_0 and θ_1 by the angle of deviation is non-linear and can not be expressed in an explicit form. Furthermore, if the angle of deviation is too large, then it is possible that $\mathbf{R}_1$ would move to a different error contour.

The various error contour plots shown in Fig. 2 illustrate the relationship between the angle of deviation, $\arccos(\mathbf{u} \cdot \mathbf{v})$, and the difference between θ_0 and θ_1 for the rotations $\mathbf{R}_0$ and $\mathbf{R}_1$ described above. This relationship varies depending on the rotation angle θ_0 of the true rotation. For illustration purpose, the angles in Fig. 2 are all in degrees. We only need to consider cases where $\theta_0 \in [0, 180)$ deg, as those cases outside this range correspond to flipping the rotation axis to the opposite direction. In Fig. 2, if $\theta_1 - \theta_0$ results in θ_1 outside the range $[0, 180)$ deg, similar interpretation can be applied. In all of the plots in Fig. 2, we can see some contours are perfectly horizontal. They correspond to the case where $\mathbf{R}_1 = \mathbf{I}$.

For instance, in Fig. 2(a) where $\theta_0 = 40\,\text{deg}$, the straight horizontal contour corresponds to $\theta_1 - \theta_0 = -40\,\text{deg}$, i.e., $\theta_1 = 0\,\text{deg}$, so the error measure is a constant 40 deg regardless of the direction of the rotation axis $\mathbf{v}$ of $\mathbf{R}_1$. In Fig. 2, it is evident that for a given rotation angle θ_0, the error contours that are less than θ_0 are closed loops while those that are larger than θ_0 are open. The vertical line (not shown in the figure) where $\arccos(\mathbf{u}\cdot\mathbf{v}) = 90$ deg and the horizontal straight contour form a pair of lines of reflection for all the contour curves.

Each plot in Fig. 2 clearly has two valleys where the errors are small. The iso-error contour plots can therefore be used as a visualization aid to help identify the shortest path for updating the estimated θ_1 angle and $\mathbf{u}$ vector for error minimization. These plots were analyzed based on the assumption that no constraints are imposed on the rotations. In many computer vision and robotics problems, such as motion capture and articulated kinematic robot arms, there are often limits associated with the rotations on each joint or the 3D orientations of the recovered poses. For instance, human subjects cannot bend their elbows forward by more than 75 deg or backward by more than 10 deg. In other words, there are infeasible regions in the space of the elbow and other joint angles of the human subjects. As a result, the iso-error contours for the recovered rotations at these joints would be disjoint curve segments.

A motivation behind the study of iso-error contours above is to find ways to reduce the search space for the estimated rotation and to make applications, such as markerless motion capture, more efficient. We note that one of the approaches commonly adopted in markerless motion capture is particle filter based (see, e.g., [2]). The particle filter is known to be an expensive visual tracking process where a large number of particles must be used in order for the tracking to be successful. The high dimensionality of the joint configuration further escalates the number of particles required. If it is known that the estimated rotation of a particular joint is more likely to have an error of, say, ϵ deg, then, knowledge of the iso-error contours of the 3D rotation of the joint is useful for reducing the sampling region for the rotation and consequently fewer particles would be necessary.

6 Conclusion

3D rotations are common entities that arise in many computer vision, graphics, and robotics problems. We have reported six functions for estimating the *distance* between two given rotations represented in various forms. Based on the well-founded theory behind 3D rotations, our detailed comparison on these functions shows that five of these functions are bi-invariant metrics, all of which respect the topology on $SO(3)$; however, only four of them are boundedly equivalent to each other. From our brief analysis on the computational complexity, we conclude that it is both spatially and computationally more efficient to use the unit quaternions for 3D rotations. We have also illustrated the geometry associated with iso-error contours and discuss its possible applications in some common computer vision problems.

Acknowledgements The author would like to thank Bill Moran for many valuable discussions on the theory of Lie groups and the anonymous reviewers for their suggestions for improving the manuscript.

Appendix A: Extracting u and θ from R

If $\mathbf{R}$ has rotation axis $\mathbf{u}$ and rotation angle θ, then $\mathbf{R}^\top$ has rotation axis $\mathbf{u}$ and rotation angle $-\theta$. From Rodrigues formula, we have

$$\mathbf{R} = \cos\theta\,\mathbf{I} + \sin\theta\,[\mathbf{u}]_\times + (1-\cos\theta)\mathbf{u}\mathbf{u}^\top, \tag{36}$$

$$\mathbf{R}^\top = \cos\theta\,\mathbf{I} - \sin\theta\,[\mathbf{u}]_\times + (1-\cos\theta)\mathbf{u}\mathbf{u}^\top. \tag{37}$$

Subtracting these two equations gives $\mathbf{R}-\mathbf{R}^\top = 2\sin\theta[\mathbf{u}]_\times$. This is a skew-symmetric matrix, from which the rotation axis can be easily extracted and normalized to unit magnitude. From the normalization, we implicitly assume that $\sin\theta \geq 0$, thus restricting $0 \leq \theta \leq \pi$. If $\mathbf{R} - \mathbf{R}^\top = \mathbf{0}$, then (i) $\mathbf{R}$ must be the identity matrix, in which case, θ can be set to 0 and $\mathbf{u}$ can be any arbitrary vector; (ii) θ must be equal to π, in which case, $\mathbf{R}+\mathbf{I} = 2\mathbf{u}\mathbf{u}^\top$ is a rank-1 matrix and $\mathbf{u}$ can be obtained by normalizing any column of $\mathbf{R}+\mathbf{I}$.

The three eigenvalues of $\mathbf{R}$ are 1 and $\exp(\pm i\theta)$. Thus, $\text{tr}(\mathbf{R}) = 1 + 2\cos(\theta)$. It follows that $\theta = \arccos((\text{tr}(\mathbf{R}) - 1)/2)$.

Computing the rotation axis and angle this way will ensure that the rotation angle is always positive and in the range $[0, \pi]$. The sign of the rotation axis is correctly determined from the normalization to suit the sign of the rotation angle.

Appendix B: Proof that Φ_6 is a Metric

To prove that Φ_6 is a metric, we show that it satisfies the three axioms listed in Sect. 3.1. Since $\Phi_6 = 2\Phi_3$ as shown in (34), it is useful to use Φ_3 in the proof when convenient.

Let $\mathbf{R}_1$, $\mathbf{R}_2$, and $\mathbf{R}_3$ be three arbitrary rotation matrices in $SO(3)$ and let their corresponding unit quaternions be denoted by $\mathbf{q}_1$, $\mathbf{q}_2$, and $\mathbf{q}_3$. Suppose that $\mathbf{R}_1\mathbf{R}_2^\top = \exp([\theta\mathbf{u}]_\times)$, where θ is the rotation angle and $\mathbf{u}$ is the unit vector representing the rotation axis. We have

$$\Phi_6(\mathbf{R}_1, \mathbf{R}_2) = 0$$

$$\Leftrightarrow \quad \|\log(\mathbf{R}_1\mathbf{R}_2^\top)\| = 0$$

$$\Leftrightarrow \quad \| [\theta \mathbf{u}]_\times \| = 0$$

$$\Leftrightarrow \quad \theta = 0 \ldots \Phi_6 \text{ returns values in the range } [0, \pi)$$

$$\Leftrightarrow \quad \mathbf{R}_1 \mathbf{R}_2^\top = \mathbf{I} \ldots \text{ obvious from Rodrigues formula (36)}$$

$$\Leftrightarrow \quad \mathbf{R}_1 = \mathbf{R}_2.$$

Φ_6 thus satisfies Axiom (i). The proof for satisfying Axiom (ii) is even more trivial:

$$\begin{aligned}\Phi_6(\mathbf{R}_1, \mathbf{R}_2) &= \| \log(\mathbf{R}_1 \mathbf{R}_2^\top) \| \\ &= \| \log(\mathbf{R}_2 \mathbf{R}_1^\top) \| \quad \ldots \text{Corollary 1} \\ &= \Phi_6(\mathbf{R}_2, \mathbf{R}_1).\end{aligned}$$

To show that the triangle inequality is also satisfied, it is easier to use Φ_3 instead:

$$\begin{aligned}&\Phi_6(\mathbf{R}_1, \mathbf{R}_3) = 2\Phi_3(\mathbf{q}_1, \mathbf{q}_3) \\ &= 2 \arccos(|\mathbf{q}_1 \cdot \mathbf{q}_3|) \\ &\leq 2 \arccos(|\mathbf{q}_1 \cdot \mathbf{q}_2|) + 2 \arccos(|\mathbf{q}_2 \cdot \mathbf{q}_3|) \\ &\qquad \ldots \text{holds for angles among unit vectors} \\ &= 2\Phi_3(\mathbf{q}_1, \mathbf{q}_2) + 2\Phi_3(\mathbf{q}_2, \mathbf{q}_3) \\ &= \Phi_6(\mathbf{R}_1, \mathbf{R}_2) + \Phi_6(\mathbf{R}_2, \mathbf{R}_3).\end{aligned}$$

References

1. Craig, J.J.: Introduction to Robotics: Mechanics and Control. Addison Wesley, Reading (1986)
2. Deutscher, J., Davison, A.J., Reid, I.: Automatic partitioning of high dimensional search spaces associated with articulated body motion capture. In: Proc. IEEE Conf. on Computer Vision and Pattern Recognition, vol. 2, pp. 669–676 (2001)
3. Faugeras, O.D., Toscani, G.: The calibration problem for stereo. In: Proc. IEEE Conf. on Computer Vision and Pattern Recognition, pp. 15–20. Miami Beach, Florida, USA (1986)
4. Heeger, D.J., Jepson, A.: Simple method for computing 3D motion and depth. In: Proc. International Conference on Computer Vision, pp. 96–100 (1990)
5. Horn, B.K.P.: Closed form solution of absolute orientation using unit quaternions. J. Opt. Soc. Am. **4**(4), 629–642 (1987)
6. Huynh, D.Q., Heyden, A.: Scene point constraints in camera autocalibration: an implementational perspective. Image Vis. Comput. **23**(8), 747–760 (2005)
7. Kelly, J.L.: General Topology. Van Nostrand, New York (1955)
8. Knight, J., Reid, I.: Automated alignment of robotic pan-tilt camera units using vision. Int. J. Comput. Vis. **68**(3), 219–237 (2006)
9. Kuffner, J.J.: Effective sampling and distance metrics for 3D rigid body path planning. In: Proc. International Conference on Robotics and Automation (2004)
10. Larochelle, P.M., Murray, A.P., Angeles, J., A distance metric for finite sets of rigid-body displacement in the polar decomposition. ASME J. Mech. Des. **129**, 883–886 (2007)
11. McCarthy, J.M.: An Introduction to Theoretical Kinematics. MIT Press, Cambridge (1990)
12. Munkres, J.R.: Topology: A First Course. Prentice-Hall, New York (1975)
13. Park, F.C.: Distance metrics on the rigid-body motions with applications to mechanism design. ASME J. Mech. Des. **117**, 48–54 (1995)
14. Park, F.C., Ravani, B.: Smooth invariant interpolation of rotations. ACM Trans. Graph. **16**(3), 277–295 (1997)
15. Pervin, E., Webb, J.: Quaternions in computer vision and robotics. In: Proc. IEEE Conf. on Computer Vision and Pattern Recognition, pp. 382–383. Los Alamitos, CA (1983)
16. Ravani, B., Roth, B.: Motion synthesis using kinematic mappings. ASME J. Mech. Transm. Autom. Des. **105**, 460–467 (1983)
17. Shoemake, K.: Animating rotation with quaternion curves. SIGGRAPH **19**(3), 245–254 (1985)
18. Watt, A., Watt, M.: Advanced Animation and Rendering Techniques. Addison Wesley, Reading (1992)
19. Wolfram MathWorld. http://mathworld.wolfram.com/EulerAngles.html
20. Wunsch, P., Winkler, S., Hirzinger, G.: Real-time pose estimation of 3D objects from camera images using neural networks. In: Proc. International Conference on Robotics and Automation, vol. 4, pp. 3232–3237 (1997)
21. Zisserman, A., Beardsley, P.A., Reid, I.: Metric calibration of a stereo rig. In: Proc. IEEE Workshop on Representations of Visual Scenes, pp. 93–100. Boston, USA (1995)

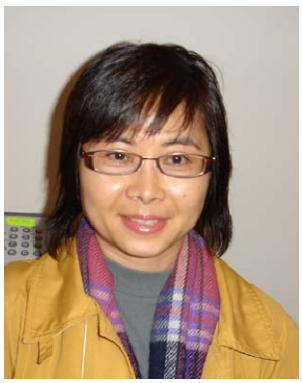

Du Q. Huynh is an Associate Professor at the School of Computer Science and Software Engineering, The University of Western Australia. She obtained her PhD in Computer Vision in 1994 at the same university. Since then, she has worked for the Australian Cooperative Research Centre for Sensor Signal and Information Processing (CSSIP) and Murdoch University. She has been a visiting scholar at Chinese University of Hong Kong, Malmö University, Gunma University, and The University of Melbourne. Associate Professor Huynh is currently a recipient of a Discovery Project grant and two Linkage Project grants funded by the Australian Research Council. Her research interests include shape from motion, multiple view geometry, video image processing, visual tracking, and signal processing.